

A NOVEL LOW PASS FILTER USING ELLIPTIC SHAPE DEFECTED GROUND STRUCTURE

X. Q. Chen, R. Li, S. J. Shi, Q. Wang, L. Xu, and X. W. Shi

National Key Laboratory of Antennas and Microwave Technology
Xidian University
Xi'an 710071, Shaanxi, China

Abstract—This paper presents a novel elliptic shape defected ground structure (DGS) for low pass filter (LPF) applications. An equivalent RLC circuit model is presented and its corresponding parameters are also extracted from the measured S-parameters. The filter presents the advantages of compact size, high selectivity; low insertion loss and high out-band suppression from 5.15 GHz to 10 GHz below -31 dB. Good agreement with response of equivalent circuit, electromagnetic simulation, and measurement is demonstrated

1. INTRODUCTION

Recently, defected ground structure (DGS) has become one of the most interesting areas of research in microwave and millimeter wave applications [1]. It could be widely used in microwave circuit design such as power divider, power amplifier and especially in filter design [1–9]. Low pass filters (LPF) design require that both in-band and out-band performances should be: low loss, high selectivity, high rejection, and wide spurious free frequency ranges. Many novel types of microstrip filters have been proposed and designed. Periodic or non-periodic DGS are realized by etching a slot in the backside metallic ground plane. The etched slot disturbs effectively the current distribution in the ground plane of microstrip line and the results in resonant characteristics [10, 11].

DGS combined with microstrip line causes a resonant character of the structure transmission with a resonant frequency controllable by changing the shape and size of the slot. There is a huge evolution in terms of defected shapes: dumbbell, periodic, fractal, circular, spiral, and L shaped [12–14]. In this paper, a novel elliptic shape DGS is

proposed for the LPF design. The use of elliptic shape DGS will be shown to give sharp cut off frequency response as well as a good performance in both the passband and the stopband. The analysis of the dimension parameters with different dimension parameters was demonstrated as a design guide. The equivalent circuit (EC) has been extracted to characterize the proposed low-pass filter. The equivalent circuit model agrees with the field simulation results. The theoretical and measured results are presented with good agreement for LPF fabrication.

2. ELLIPTIC SHAPE DGS LOW PASS FILTER

2.1. DGS Cell and Equivalent Circuit

The proposed DGS cell is obtained by etching a slot connecting with two elliptic shapes defected structure in the ground plane, as shown in Figure 1. The width of microstrip line on the top is 1.88 mm, which corresponds to $50\ \Omega$ characteristic impedance. And its equivalent circuit of the cell is proposed. To derive the equivalent network parameters, the S-parameters of a DGS cell at the reference plane should be calculated using EM-simulator. And then, by using the relationship between the S parameter, the equivalent network parameters can be extracted as follows [11]:

$$C = \frac{\omega_c}{2Z_0(\omega_0^2 - \omega_c^2)} \quad (1)$$

$$L = \frac{1}{4(\pi f_0)^2 C} \quad (2)$$

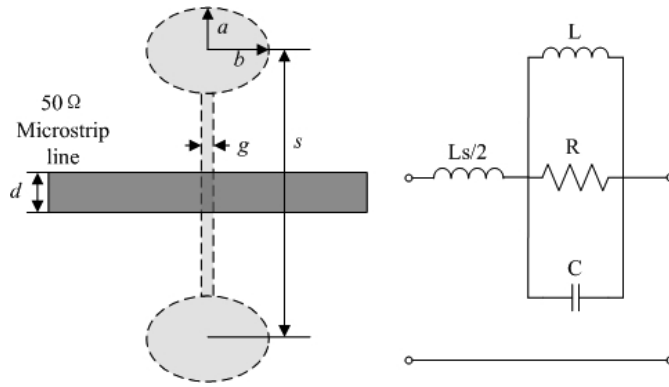


Figure 1. The proposed elliptic DGS cell and its equivalent circuit.

$$R = \frac{2Z_0}{\sqrt{\frac{1}{|S_{11}(\omega_0)|^2} - \left(2Z_0 \left(\omega_0 C - \frac{1}{\omega_0 L}\right)\right)^2} - 1} \quad (3)$$

where ω_0 is the angular resonance frequency, ω_c is the 3-dB cutoff frequency, and Z_0 is the characteristic impedance of the microstrip transmission line.

As it is known, there is a close relationship between the etched shapes of the DGS and its frequency characteristics. Here a comparison between three types of DGS structure including dumbbell, circular and elliptic shape were carried out and simulated to identify their characteristics. The DGS cells have been simulated using HFSS and the permittivity of the dielectric board is 3.2 and the thickness h is 0.787 mm. For the comparison study of the properties, three types of DGS cell have the same defected areas of 15.1 mm^2 , slot length $s = 12 \text{ mm}$ and slot width $g = 0.2 \text{ mm}$, where the elliptic shape with radius $a = 2 \text{ mm}$ and $b = 2.4 \text{ mm}$ was replace by circular shape with radius of 2.19 mm and dumbbell shape with square length of 3.88 mm. Figure 2 shows the similar characteristic curves of the proposed DGS cell.

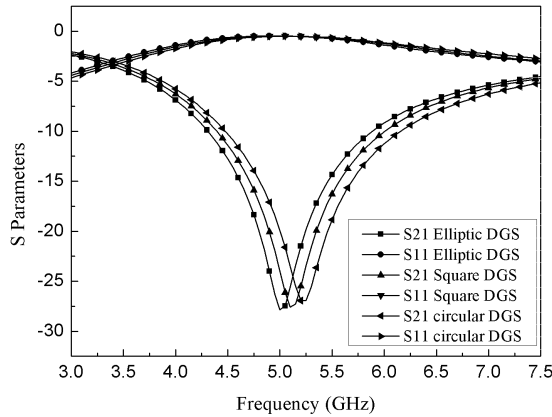


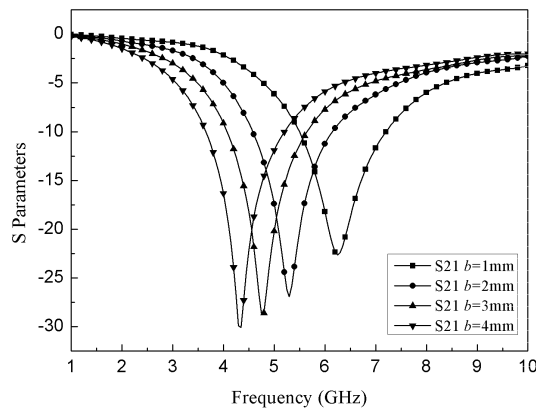
Figure 2. Comparison of three types of DGS cell of elliptic, dumbbell and circular shapes.

The results for three types of DGS including dumbbell, circular and elliptic shape were summarized in Table 1. As Table 1 shown, the cutoff frequency changes slightly, while the resonance frequency of the proposed DGS is smaller than that of the other two types. And the sharper cutoff frequency and slow wave performance could be obtained by using the elliptic DGS.

Table 1. Comparison of characteristic of DGS cell.

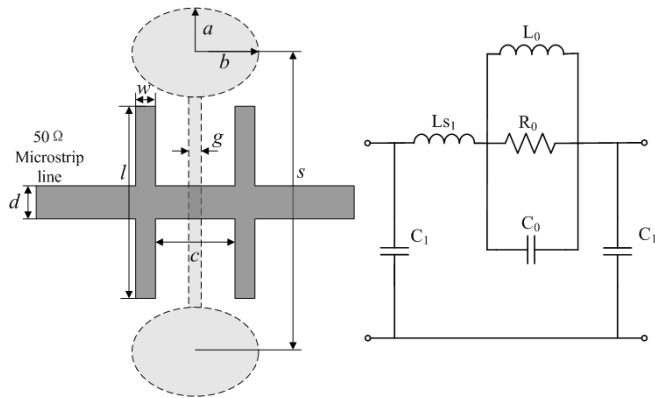
	Elliptic	Dumbbell	Circular
f_c (GHz)	3.25	3.32	3.44
f_0 (GHz)	5.01	5.12	5.18
L (nH)	2.833	2.579	2.581
C (pF)	0.358	0.375	0.366
S_{21max} (dB)	-27.85	-27.58	-26.93

For the elliptic DGS cell, its resonant characteristics are mainly affected by its radius a and b . Figure 3 shows the frequency responses of EM simulation for the elliptic DGS with different radius b . The radius b varies from 1 mm to 4 mm, while radius $a = 2$ mm, slot length $s = 12$ mm, slot width $g = 0.2$ mm are constant. The variation of the characteristics could be explained by its equivalent circuit model. It demonstrates that the value of the equivalent inductance L increases as the radius b increasing from 1 mm to 4 mm, while has relatively little effect on the equivalent capacitance C . And the attenuation pole shifts from 6.28 GHz to 4.32 GHz. This causes the equivalent inductance increases proportion to the areas of the defected rectangle. And these make well explain for the shift of the cutoff frequency and the attenuation poles with changing the dimension parameters of the DGS which closely affect the values of the equivalent parameters.

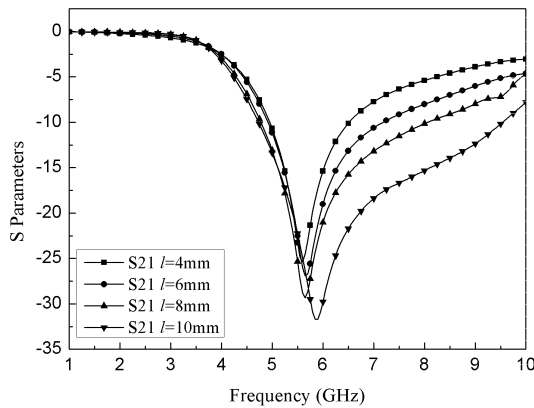
**Figure 3.** Frequency characteristic of the proposed DGS cell with different radius b .

2.2. Low-Pass Filter Design and Optimization

As analyzed above, the elliptic DGS can be used for low-pass filter design and spurious passband suppression. However, this structure also has some disadvantages such as insufficient suppression in high frequency range and slow cutoff characteristic. Therefore, an H shape open stubs are used in the single DGS cell to increase coupling capacitance between the microstrip line and the elliptic DGS which could minimize the size of the LPF and improve the stopband performance. Figure 4(a) shows proposed structure the LPF with H shape open stubs which parameters are $c = 2.6 \text{ mm}$, $w = 1 \text{ mm}$,



(a)



(b)

Figure 4. Improved elliptic DGS cell (a) DGS cell with H shape stub, (b) Frequency response with stub length l from 4 mm to 10 mm.

$a = 1$ mm, $b = 1.5$ mm and $d = 1.88$ mm as constant. Figure 4(b) shows the simulated results with stub length l varies from 4 mm to 10 mm. As open stub length l increased, the equivalent parallel capacitance C_1 increases and the outband suppression could be improved and the attenuation pole is deeper without changing the 3 dB cutoff frequency at 3.98 GHz. And the outband suppression was improved about 15 dB when the stub length l of 10 mm compared with 4 mm.

To design the desired low pass filter and improve the out band suppression, more DGS cells should be increased. The proposed low pass filter with optimized dimensions based on the analysis of single cells was proposed with its equivalent circuit as Figure 5 shown. The dimension parameters are all constant except the open stub l_2 . The value of the parameters are $a = 1$ mm, $b = 1.5$ mm, $b_1 = 2$ mm, $w = 1$ mm, $g = 0.2$ mm, $s_1 = 12$ mm, $s_2 = 6$ mm, $l_1 = 10$ mm, $l_3 = 5$ mm and $l_4 = 8$ mm.

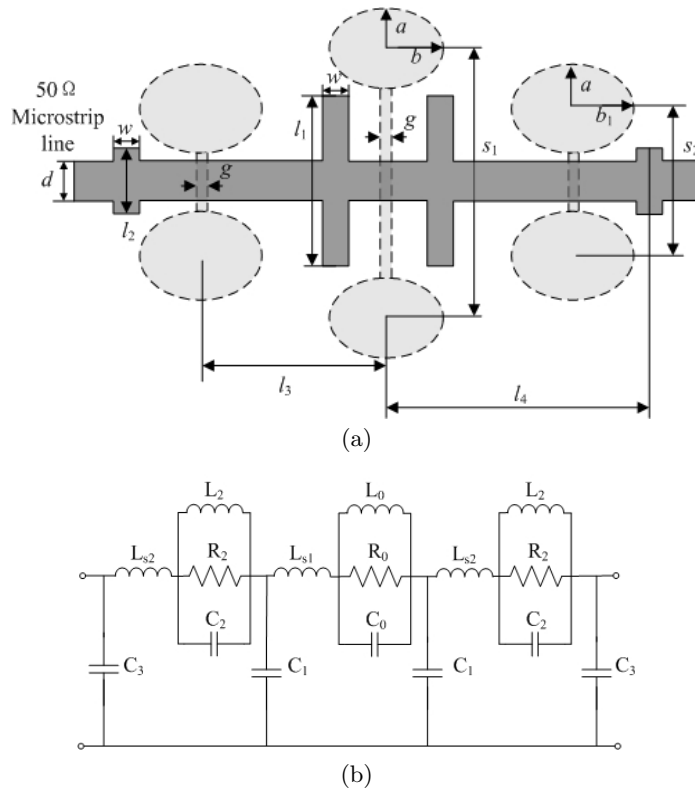


Figure 5. The proposed LPF (a) LPF with elliptic DGS, (b) Equivalent circuit network.

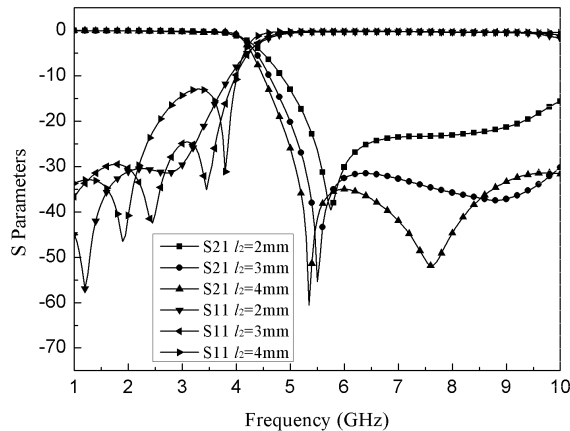


Figure 6. Simulated results of the proposed LPF with varied l_2 .

Figure 6 shows the simulated results of proposed low pass filter with different length of the open stub l_2 . When the length of stub l_2 increases, its parallel equivalent capacitance C_3 which is shown in Figure 5(b) increases too. The increased of C_3 makes the out-band suppression become lower which improves from -25 dB to -37 dB and the passband to stopband attenuation slope become sharper. While it is note that the in-band performances including insertion loss and return loss get worse at the same time. So the performances both of the passband and stopband should be concerned at the same time, and the tradeoff design method should be taken.

It means that the equivalent parallel capacitance C_3 should be chosen properly. So the parameters of the low-pass filter could be controlled and optimized by adjusting the stub length l_2 with proper length. The EM and the EC simulated results of the LPF with optimized dimensions $l_2 = 3$ mm based on three elliptic DGS cell was proposed as shown in Figure 7. These values of parameter in the equivalent network are: $C_0 = 0.43$ pF, $L_0 = 2.21$ nH, $R_0 = 2.192$ k Ω , $C_2 = 0.21$ pF, $L_2 = 0.93$ nH, $R_2 = 1.642$ k Ω , $L_{s1} = 1.13$ nH, $L_{s2} = 2.38$ nH, $C_1 = 1.41$ pF and $C_3 = 0.56$ pF. The validity of the EM and EC simulated has a good agreement and shows the validity of the EC model simulation by Advanced Design System (ADS). The return losses throughout passband range are below -24 dB, while out-band suppression are generally more than 32 dB at a wide range from 5.17 GHz to 10 GHz. The use of open stubs achieves larger attenuation in the stopband and obtains higher harmonic suppressions with less number of periodic structures compared to the conventional DGS filter.

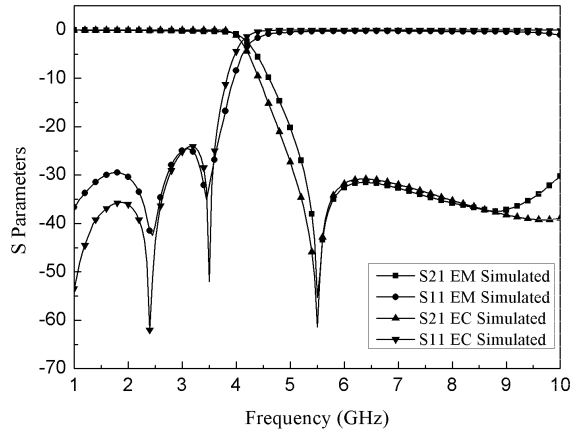
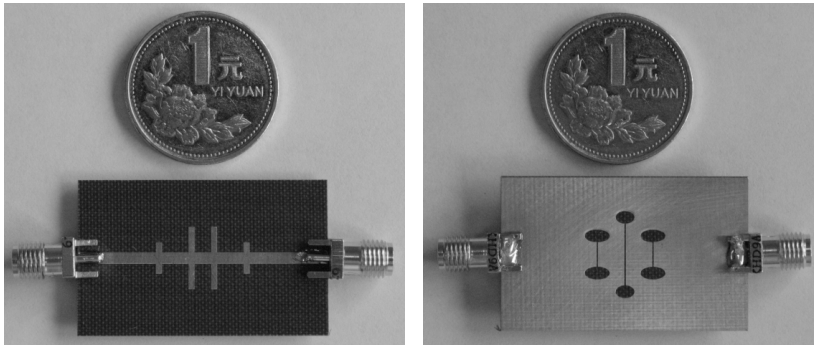


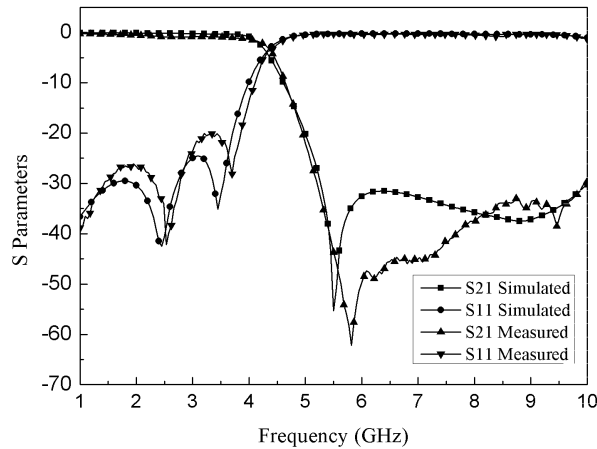
Figure 7. The proposed LPF with EM and EC simulated results.

3. IMPLEMENTATION AND RESULTS

To validate the proposed low pass filter, it was simulated and fabricated with Taconic TLC which has relative a permittivity $\epsilon_r = 3.2$ and a thickness $h = 0.787$ mm. Figure 8(a) shows the photograph of the proposed low pass filter with compact size of $25 \text{ mm} \times 40 \text{ mm}$. The measured results have shown a good agreement with the theoretical results. The experiment results show that the fabricated LPF has a 3 dB cut off frequency at 4.5 GHz and there is a shift of cut off frequency about 50 MHz. The insertion loss in the passband is low and its stopband is well suppressed below -32 dB from 5.2 GHz to 10 GHz.



(a)



(b)

Figure 8. Experiment results (a) Photograph of the proposed low-pass filter, (b) comparison of the simulated and measured results.

4. CONCLUSIONS

In this paper, a novel compact microstrip low-pass filter using elliptic DGS cells is presented. The novel H shape open stub increases the equivalent parallel capacitance to improve the outband suppression. An equivalent circuit model was given to depict the novel DGS filter. The proposed structure with main dimension parameters was analyzed as a design guide to fabricate the filter. The measurement results have shown good agreement with the theoretical results. The proposed LPF has sharp cut off frequency response, low insertion loss, and good rejection in stopband from 5.17 GHz to 10 GHz which was suppressed below -32 dB.

REFERENCES

1. Park, J., J. P. Kim, and S. Nam, "Design of a novel harmonic-suppressed microstrip low-pass filter," *IEEE Microw. Wirel. Compon. Lett.*, Vol. 17, No. 6, 424–426, 2007.
2. Shobeyri, M. and M. H. Vadjed-Samiei, "Compact ultra-wideband bandpass filter with defected ground structure," *Progress In Electromagnetics Research Letters*, Vol. 4, 25–31, 2008.
3. Naghshvarian-Jahromi, M. and M. Tayarani, "Miniature planar

- UWB bandpass filters with circular slots in ground,” *Progress In Electromagnetics Research Letters*, Vol. 3, 87–93, 2008.
4. Oraizi, H. and M. S. Esfahlan, “Miniaturization of Wilkinson power dividers by using defected ground structures,” *Progress In Electromagnetics Research Letters*, Vol. 4, 113–120, 2008.
 5. Chen, X.-Q., X.-W. Shi, Y.-C. Guo, and M.-X. Xiao, “A novel dual band transmitter using microstrip defected ground structure,” *Progress In Electromagnetics Research Letters*, Vol. 4, 113–120, 2008.
 6. Oskouei, H. D., K. Forooghi, and M. Hakkak, “Guided and leaky wave characteristics of periodic defected ground structures,” *Progress In Electromagnetics Research*, PIER 73, 15–27, 2007.
 7. Chen, J., Z.-B. Weng, Y.-C. Jiao, and F.-S. Zhang, “Lowpass filter design of Hilbert curve ring defected ground structure,” *Progress In Electromagnetics Research*, PIER 70, 269–280, 2007.
 8. Sharma, R., T. Chakravarty, S. Bhooshan, and A. B. Bhattacharyya, “Design of a novel 3 db microstrip backward wave coupler using defected ground structure,” *Progress In Electromagnetics Research*, PIER 65, 261–273, 2006.
 9. Zhang, F. and C. F. Li, “Power divider with microstrip electromagnetic bandgap element for miniaturisation and harmonic rejection,” *Electron. Lett.*, Vol. 44, No. 6, 422–424, 2008.
 10. Hong, J. S. and B. M. Karyapudi, “A general circuit model for defected ground structure’s in planar transmission lines,” *IEEE Microw. Wirel. Compon. Lett.*, Vol. 15, No. 10, 706–708, 2005.
 11. Ahn, D., J. S. Park, C. S. Kim, J. Kim, Y. X. Qian, and T. Itoh, “A design of the low-pass filter using the novel microstrip defected ground structure,” *IEEE Trans. Microw. Theory Tech.*, Vol. 49, No. 1, 86–93, 2001.
 12. Boutejdar, A., A. Elsherbini, and A. Ornar, “Design of a novel ultra-wide stopband lowpass filter using h-defected ground structure,” *Microw. Opt. Technol. Lett.*, Vol. 50, No. 3, 771–775, 2008.
 13. Piscarreta, D. and S. W. Ting, “Microstrip parallel coupled-line bandpass filter with selectivity improvement using u-shaped defected ground structure,” *Microw. Opt. Technol. Lett.*, Vol. 50, No. 4, 911–915, 2008.
 14. Xiao, J. K., S. W. Ma, S. Zhang, and Y. Li, “Novel compact split ring stepped-impedance resonator (sir) bandpass filters with transmission zeros,” *J. Electromagn. Waves Appl.*, Vol. 21, No. 3, 329–339, 2007.